Signaling between periglomerular cells reveals a bimodal role for GABA in modulating glomerular microcircuitry in the olfactory bulb

Pirooz Victor Parsa[a,b], Rinaldo David D'Souza[a,b,1], and Sukumar Vijayaraghavan[a,b,2]

[a]Department of Physiology and Biophysics, University of Colorado School of Medicine, Aurora, CO 80045 and [b]Neuroscience Program, University of Colorado School of Medicine, Aurora, CO 80045

Edited by Charles F. Stevens, The Salk Institute for Biological Studies, La Jolla, CA, and approved June 23, 2015 (received for review December 22, 2014)

In the mouse olfactory bulb glomerulus, the GABAergic periglomerular (PG) cells provide a major inhibitory drive within the microcircuit. Here we examine GABAergic synapses between these interneurons. At these synapses, GABA is depolarizing and exerts a bimodal control on excitability. In quiescent cells, activation of $GABA_A$ receptors can induce the cells to fire, thereby providing a means for amplification of GABA release in the glomerular microcircuit via GABA-induced GABA release. In contrast, GABA is inhibitory in neurons that are induced to fire tonically. PG–PG interactions are modulated by nicotinic acetylcholine receptors (nAChRs), and our data suggest that changes in intracellular calcium concentrations triggered by nAChR activation can be amplified by GABA release. Our results suggest that bidirectional control of inhibition in PG neurons can allow for modulatory inputs, like the cholinergic inputs from the basal forebrain, to determine threshold set points for filtering out weak olfactory inputs in the glomerular layer of the olfactory bulb via the activation of nAChRs.

nicotinic | excitatory GABA | interneurons | cholinergic | normalization

The balance of excitation and inhibition is critical for the normal functioning of brain networks. Timed inhibition of principal neurons modulates circuit output and contributes to network synchrony and oscillation. GABAergic interneurons play a key role in regulating these network properties (1, 2). Recent findings (e.g., ref. 3), however, have compelled us to move away from a simple view of transmission in the brain, in which glutamate and GABA represent the major excitatory and inhibitory transmitter systems, to a more nuanced interpretation of their roles.

GABAergic neurotransmission has both inhibitory and excitatory effects in the CNS. Whereas the inhibitory actions of GABA on principal neurons in different brain regions have been examined extensively, studies of excitatory GABA have focused mostly on the developmental aspects of neuronal growth and synapse formation (4, 5). Recent evidence suggests that GABA can be excitatory in mature neurons as well (with the term "mature" here referring to neurons that are integral parts of established brain networks) (3, 6).

Dynamic GABAergic signaling between inhibitory interneurons is less well understood. The common assumption is that GABAergic signaling between these interneurons would lead to disinhibition of principal neurons in a circuit. Excitatory GABA signaling between these interneurons, on the other hand, could serve as a means for amplification of principal cell inhibition. A combination of the two could effectively buffer interneuron firing rates and possibly normalize circuit output in a given area (7).

The modularity in brain circuits allows for application of principles gleaned from the study of one defined circuit to other circuits as well. In the olfactory bulb (OB) glomerulus, the GABAergic periglomerular (PG) cells provide a large fraction of the inhibitory drive for information transfer between the olfactory nerve (ON) and mitral cells (MCs), the principal neurons. In this system, the existence of PG–PG synapses has been demonstrated (8), and GABA has been suggested to be depolarizing, yet inhibitory, on these neurons (9). Whether these synapses participate in glomerular signaling either during odor input or during neuromodulation of glomerular output is not yet known.

In this paper, we report that GABAergic connections between PG cells have a bimodal effect on excitation depending on the previous activity state of the neurons. Excitation of PG cells by GABA can lead to amplification of glomerular inhibition via GABA-induced GABA release (GIGR). GABA release from PG cells modulates glomerular output on the activation of nicotinic acetylcholine receptors (nAChRs), wherein weak signals from the ON are filtered out while stronger ones are transmitted (10). Our results suggest that bimodal signaling by GABA could be important in determining set points for inhibition thresholds in the glomerular microcircuit.

Results

GABA Type A Receptor Activation Raises Intracellular Free Calcium Levels. We first tested whether GABA was depolarizing in a population of juxtaglomerular (JG) neurons. Slices were loaded with fura-2AM. To isolate GABAergic signals, loaded slices were incubated with glutamate receptor (GluR) blockers [10 μM 6,7-dinitroquinoxaline-2,3-dione (DNQX), 50 μM (2*R*)-amino-5-phosphonopentanoate (APV), and 500 μM (*S*)-α-methyl-4-carboxyphenylglycine (MCPG), to block AMPA and NMDA receptors and metabolic GluRs, respectively] and TTx. GABA (100 μM–1 mM) was applied locally via a puffer pipette. Calcium signals were monitored from JG neurons.

Brief (1–5 s) application of GABA to OB glomeruli from 12- to 18-d-old mice resulted in rapid calcium transients (Fig. 1*A*, *i*).

Significance

Excitation-driven inhibition is one mechanism for manipulating gain control in brain microcircuits. Here we show that interactions between GABAergic interneurons in the glomerulus in the olfactory bulb can, in a dynamic fashion, regulate inhibition of circuit output. GABA is depolarizing on these interneurons; however, depending on the activity state of these neurons, it can be excitatory or inhibitory, thereby providing a bimodal regulation of inhibition. In the olfactory bulb, activation of nicotinic acetylcholine receptors can drive glutamate-dependent GABAergic mechanisms that allow for timed filtering of incoming inputs. These mechanisms can serve to normalize inhibition across the glomerular layer by cholinergic activation, taking into account both behavioral states and the activity history of individual glomeruli.

Author contributions: P.V.P., R.D.D., and S.V. designed research; P.V.P. and R.D.D. performed research; P.V.P., R.D.D., and S.V. analyzed data; and P.V.P., R.D.D., and S.V. wrote the paper.

The authors declare no conflict of interest.

This article is a PNAS Direct Submission.

[1]Present address: Department of Anatomy and Neurobiology, Washington University School of Medicine, St. Louis, MO 63110.

[2]To whom correspondence should be addressed. Email: sukumar.v@ucdenver.edu.

This article contains supporting information online at www.pnas.org/lookup/suppl/doi:10.1073/pnas.1424406112/-/DCSupplemental.

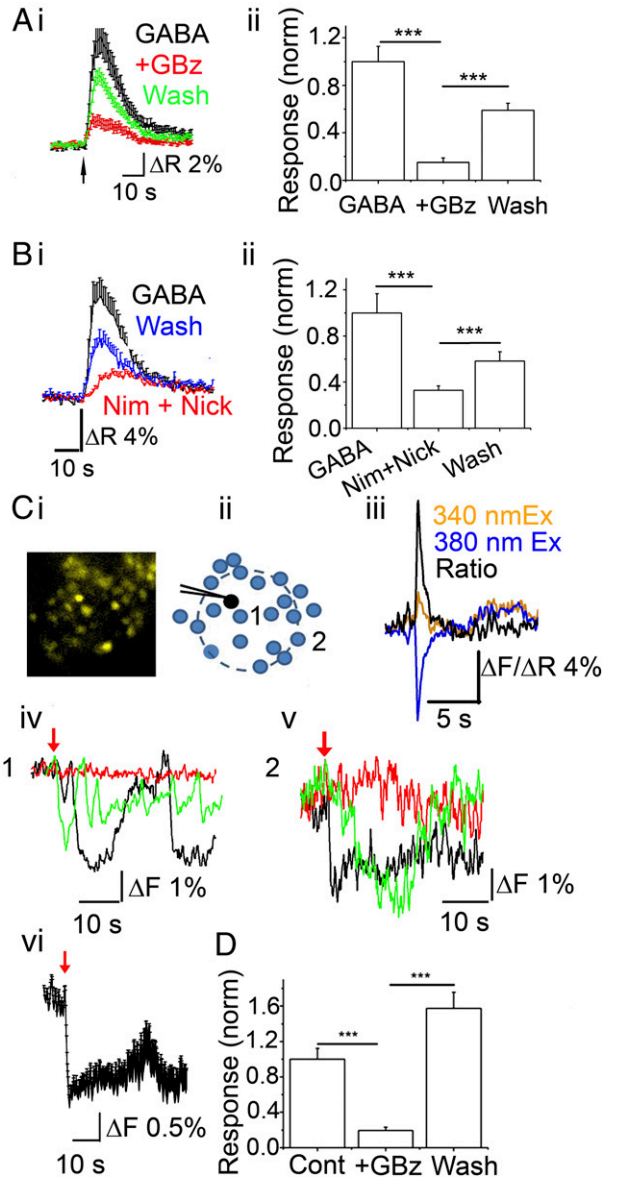

Fig. 1. Both exogenous and endogenous GABA induce $GABA_A$ receptor-mediated calcium transients in a population of JG neurons. (*A*) (*i*) Averaged trace (± SEM) of calcium transients from JG neurons in response to a 5-s application of 1 mM GABA in the presence of 1 μM TTX, 50 μM DNQX, and 100 μM APV. Black, GABA; red, in the presence of 20 μM GBz (+GBz); green, wash. (*ii*) Data quantification from *i* ($n = 63$ cells from four experiments). GBz potently inhibited GABA-induced calcium transients ($P < 10^{-8}$ compared with GABA alone, paired *t* test), which was reversed on washout of the antagonist ($P < 10^{-7}$ compared with +GBz). (*B*) (*i*) A 5-s application of 1 mM GABA triggers VGCC-dependent calcium transients in a population of JG neurons. Average trace (± SEM) from control (GABA; black), in the presence of 20 μM nimodipine and 500 μM nickel (Nim + Nick; red), and wash (blue). (*ii*) Quantification of data ($n = 51$ cells, three experiments; $P < 0.001$ for GABA and wash compared with Nim + Nick). ***$P < 0.0005$, paired *t* test. (*C* and *D*) Calcium transients in response to depolarization of a single PG cell. (*C*) Fura-2AM–loaded cells were imaged before and after delivery of a single 100-ms voltage step to a PG neuron in the presence of 10 μM DNQX and 50 μM APV. (*i*) Image of a fura-2AM–loaded glomerulus. (*ii*) Cartoon depicting the recorded PG cell (black) and surrounding JG cells that respond with calcium transients to the depolarizing step (blue). (*iii*) Calcium transient from the patched PG cell (loaded with 200 μM bis-fura-2 hexapotassium salt) on a 100-ms voltage step. The orange trace represents changes from the 340-nm excitation; blue trace, changes from the 380-nm excitation; black trace, changes in the 340 nm/380 nm ratio. (*iv*) Changes in fluorescence from 380-nm excitation from a single cell (cell labeled 1 in *D*) eliciting an oscillatory calcium transient on PG cell depolarization alone (black), in the presence of 20 μM GBz (red), and wash (green). (*v*) Fluorescence from 380-nm excitation changes from another cell (cell labeled 2 in *D*) eliciting a calcium transient on PG cell depolarization (black), in the presence of 20 μM GBz (red), and wash (green). (*vi*) Average response (± SEM) from all responding cells ($n = 21$) in the glomerulus. (*D*) Data from four independent experiments. Cells surrounding the patched PG neuron show calcium transients that are blocked by 20 μM GBz (+GBz; $P < 0.0001$). On washout, the response recovered ($P < 0.0001$, compared with +GBz).

Incubating the slices with 20 μM gabazine (GBz) reduced the fluorescence (integrated over the response) to 15 ± 3.7% of the control responses ($n = 63$ cells from three experiments; $P < 10^{-8}$, paired *t* test) which was partially reversed (to 55 ± 6% of the control response) after a 10-min washout ($n = 63$; $P < 10^{-7}$, paired *t* test compared with GBz) (Fig. 1*A*, *ii*). We then confirmed that GABA-mediated calcium transients were not unique to young mice. From five experiments, JG cells from 75- to 90-d-old mouse OBs also responded to GABA with an increase in $[Ca]_i$ (Fig. S1), indicating that age is not a determining factor.

We then confirmed that the calcium signals obtained from GABA type A receptor ($GABA_AR$) activation resulted from depolarization of the cells by testing the contribution of voltage-gated calcium channels (VGCCs). Incubating the slices with 50 μM nimodipine and 500 μM nickel reduced the calcium response to 33 ± 3% of control ($n = 51$ cells from three experiments; $P < 0.0005$; paired *t* test), which was partly reversed upon washout (Fig. 1*B*, *i* and *ii*). To confirm VGCC blockade, we measured the effects of the blockers on calcium responses to 70 mM KCl on the same cells. The VGCC antagonists reduced the response to a 1-s application of 70 mM KCl to 45 ± 3% of control ($P < 0.0005$).

Based on these results, we asked whether endogenously released GABA from PG cells could result in calcium changes in surrounding neurons, potentially via PG–PG interactions. We loaded slices with fura-2AM (Fig. 1*C*, *i*). We held PG neurons under a whole-cell voltage clamp using CsCl-based internal solutions containing 10 mM GABA, 200 μM bis-fura-2 hexapotassium salt, and 200 μM Alexa Fluor 594 hydrazide (to confirm the identity of the recorded PG cell). GluR currents were blocked using 10 μM DNQX and 50 μM AP-5. A 100-ms voltage step was applied from −70 mV to 0 mV. Images were acquired at 2–7 Hz. GBz-sensitive, slow "self-inhibitory" currents were observed following the voltage step (119 ± 42 pA; $n = 4$ cells out of 7).

We measured calcium changes from all JG neurons within a glomerulus before and for 45 s after the voltage step. Results are shown in Fig. 1*C*. Following the voltage step, surrounding JG neurons showed calcium transients. Surprisingly, responses were not confined to neurons in the vicinity of the voltage-clamped neurons, but were widespread across the glomerulus (Fig. 1*C*, *i*–*vi*). On average, 60 ± 14% of all JG neurons that were loaded with fura-2AM responded with calcium transients ($n = 4$ experiments). We did not investigate the possible spread of the signal across glomeruli in this study. The onset of the calcium response in all responding neurons occurred with a ≤1-s delay in the voltage step, suggesting fast propagation of the signal. Incubating cells with 10 μM GBz reduced the response by 87 ± 2.4% (data from four experiments; $P < 0.0001$, paired *t* test), which was reversed after 15 min of washing (Fig. 1*D*). The recovered response was 52 ± 10% larger on average than the first response ($P < 0.05$, paired *t* test). Whether this increase indicates some tonic regulation of basal calcium levels by ambient GABA remains to be investigated.

The foregoing results are consistent with the idea that GABA is depolarizing in PG cells. The surprising finding that depolarizing a single PG neuron can raise calcium levels in most JG neurons raises the possibility that GABA is excitatory and can propagate signals across PG cells.

GABA Is Excitatory on PG Cells. Smith and Jahr (9) suggested that depolarization by GABA nevertheless blocks firing in PG neurons

via shunt inhibition. To determine whether PG neurons can fire on activation of GABA receptors, we performed cell-attached recordings from PG cells using recording pipettes containing 200 μM Alexa Fluor 594 hydrazide. These cells were initially identified by their size and the fact that none of them showed spontaneous bursts of action potentials (APs), a characteristic of the glutamatergic external tufted (ET) cells. The idea that PG cells exhibit very little to no spontaneous firing is consistent with recent studies demonstrating the same in vivo (11, 12). All experiments were done in the presence of the aforementioned GluR blockers. In six out of six cells, where we successfully broke through into a whole-cell configuration, their identity was further confirmed morphologically (small size, short dendritic arbors; Fig. 2*A*). Brief applications of 25–50 μM GABA resulted in firing of PG cells (Fig. 2*A*). GABA-mediated changes in PG cell firing were completely blocked by incubating the slice in 20 μM GBz ($n = 4$). Transient GABA-induced firing in these neurons lasted an average of 3.2 ± 0.85 s, with an average frequency of 6.3 ± 2 Hz ($n = 9$ cells). An additional four cells fired one or two APs on GABA application.

Our results suggest that GABA is excitatory on these neurons; however, it is possible that GABA is inhibitory in PG cells but the cells themselves are under a tonic inhibition from other GABA-sensitive neurons. Thus, application of GABA would result in disinhibition of PG cells by removal of this tonic inhibition. Such a scenario implies that under current-clamp conditions, application of GABA should result in depolarization even under conditions in which GABA is hyperpolarizing in the recorded neuron. We performed whole-cell current-clamp recordings from PG cells, using intracellular solutions (K-gluconate based; $E_{Cl} = -108$ mV) that would make GABA hyperpolarized in the recorded cell (Fig. 2*B*). The resting membrane potential (RMP), determined immediately after going whole cell, averaged −55 ± 3 mV ($n = 7$ cells). Brief applications of 100 μM GABA resulted in no membrane depolarizations, as would be predicted if the excitatory actions of GABA arose from disinhibition of a tonically inhibited cell ($n = 5$).

We examined whether activation of the hyperpolarization activated current (I_h), known to be present in MCs (13) and a subset of PG cells (14), contributes to PG cell firing. Cell-attached recordings were carried out on PG cells in the presence and absence of 30 μM ZD 7288, an I_h blocker (15, 16). In the presence of the inhibitor, application of 25 μM GABA still elicited firing (mean firing frequency, 1.35 ± 0.37 Hz in controls vs. 2.28 ± 0.73 Hz after a 15-min treatment with ZD 7288; $n = 5$ cells; $P = 0.3$) (Fig. S2 *A* and *B*). Consistent with our current-clamp experiments (Fig. 2*B*), these results suggest that I_h activation does not drive the cells above their firing threshold. The lack of depolarization in the current-clamp recordings also makes it unlikely that other forms of rebound depolarization contribute to the excitatory effects of GABA.

Having ruled out disinhibition or rebound depolarization, we conducted measurements of the reversal potential for GABA-evoked currents (E_{GABA}) in PG cells. Perforated patch recordings were carried out using K-gluconate–based solutions containing gramicidin D (*Methods*). GABA currents were measured at various holding potentials (Fig. 2*C*). From a total of six cells, the mean E_{GABA} was calculated to be −49 ± 2 mV. RMPs were obtained from seven cells. Of these, six cells had a mean RMP of −60 ± 2 mV, and one cell had an RMP of −45 mV. This finding suggests that most PG cells rest approximately 10 mV negative to E_{GABA}, thereby making GABA depolarizing on these neurons. The observed E_{GABA} would result from an intracellular chloride concentration of approximately 19 mM, assuming that bicarbonate does not significantly affect the GABA reversal potential. This compares with intracellular chloride concentrations of 15 mM observed in cerebellar interneurons where GABA is depolarizing (7) and 25 mM in newborn hippocampal neurons (17).

In 10 cells, either with the first GABA application or after repeated application of the agonist, the originally silent neuron went into a persistent firing mode firing at an average frequency of

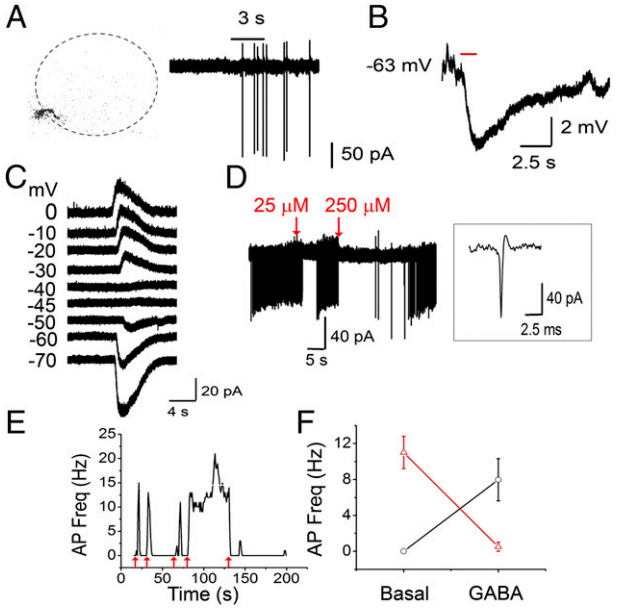

Fig. 2. Bimodal actions of excitatory GABA. (*A*) (*Left*) PG cell filled with Alexa Fluor 594 hydrazide after cell-attached recording. (*Right*) Cell-attached recording from the same cell. The cell was held at 0 holding current. A 3-s (black bar) 25 μM GABA application (in the presence of 10 μM DNQX and 50 μM APV) triggers a transient burst of APs. (*B*) A PG cell under whole-cell current-clamp (I = 0). A 1-s application of 100 μM GABA results in hyperpolarization of the membrane potential, arguing against disinhibition. No rebound depolarization was observed. The RMP was −63 mV. (*C*) Responses to a 3-s application of 50 μM GABA were recorded at various holding potentials (from −70 mV to 0 mV) using gramicidin D perforated patch recordings. E_{GABA} in this cell was at approximately −45 mV. (*D*) Long-lasting bursts of APs were triggered by application of 25 μM GABA. Firing was inhibited in response to application of both 25 μM and 250 μM GABA (red arrows) for 3 s. (*Inset*) Expanded trace showing a single event. (*E*) Frequency plot of a PG cell responding to 25 μM GABA (red arrows) either with a small burst of APs or a long burst of APs that was shunted (at the fourth arrow). Same cell as in *D*. (*F*) Average response plot of all cells representing bimodality of GABA responses. PG neurons that were silent were excited (black; $n = 6$). Neurons that were induced to fire continuously after GABA application were inhibited (red; $n = 7$).

8.9 ± 2 Hz ($n = 7$; Fig. 2 *D*–*F*) after the agonist was removed. When GABA was applied to a tonically firing PG cell, its effect was to silence the neuron for a brief period ($n = 6$; Fig. 2*F*). A 1-s application of 25–50 μM GABA transiently silenced the neuron (Fig. 2*D*), which recovered after washout of the agonist.

A parsimonious interpretation of our results (Figs. 1 and 2) is that activation of $GABA_A$Rs results in depolarization-driven calcium flux via the opening of VGCCs and drives the cell above its firing threshold. Given that it is possible to evoke both transient and continuous firing in the same PG cell, this is less likely to reflect different subpopulations of these neurons rather than differences in active conductances, including those activated by calcium entry. Whether PG cell firing, induced by previous activation of $GABA_A$Rs, provides the necessary total conductance for effective shunt inhibition or whether there are rapid changes in intracellular chloride concentrations remains to be determined. The bidirectional effect of GABA also will prevent a potential positive feedback loop that might lead to runaway excitation of the PG cell population.

GABAergic Signaling Among PG Cells via GIGR. To further demonstrate that GABA released from a PG neuron can result in amplified GABA release within the glomerular network via PG–PG interactions (i.e., GIGR), we asked whether exogenous GABA, applied at a distance, can give rise to spontaneous GABAergic postsynaptic currents (sGPSCs). A PG neuron was held under

whole-cell voltage-clamp using CsCl-based internal solutions containing 200 μM Alexa Fluor 488 dextran. Then 50 μM GABA was applied via a puffer pipette at a location distant to the recorded neuron (Fig. 3*A*, *i*). In some experiments, the puffer pipette contained Alexa Fluor 594 hydrazide to track the diffusion of the applied agonist (Fig. 3*A*, *ii*), but in most cases, whole-cell $GABA_AR$ currents at the recorded PG cell were used as indicators of distance between the recorded cell and the agonist application locus. The bath contained DNQX and APV as described above. In five cells, 0.5 mM MCPG was also added to block type 1 metabolic GluRs. Its addition did not lead to a discernible difference in outcomes, and the antagonist was omitted in other cells.

Application of GABA near the recorded PG cell resulted in a large whole-cell current blocked by 20 μM GBz. sGPSCs were superimposed on this current. Moving the application pipette further away (determined empirically) resulted in a small, delayed whole-cell current with a barrage of sGPSCs preceding it (Fig. 3*A*, *ii*). Application of GABA resulted in an 11.3 ± 3-fold increase in GPSC frequencies over basal levels (n = 23 cells; $P < 0.0001$) (Fig. 3*C*). When the puffer pipette was moved away from the recorded cell, to a location where no whole-cell currents were observed from the recorded neuron, the GPSC barrage persisted (8 ± 2-fold increase; n = 5; P = 0.39, not significantly different from cells showing direct activation by the applied GABA) (Fig. 3 *B* and *C*). The duration of the GPSC bursts was not significantly different in the two conditions (7.6 ± 0.44 s vs. 8.9 ± 1.2 s; P = 0.37, near vs. far) (Fig. 3*D*). In addition,

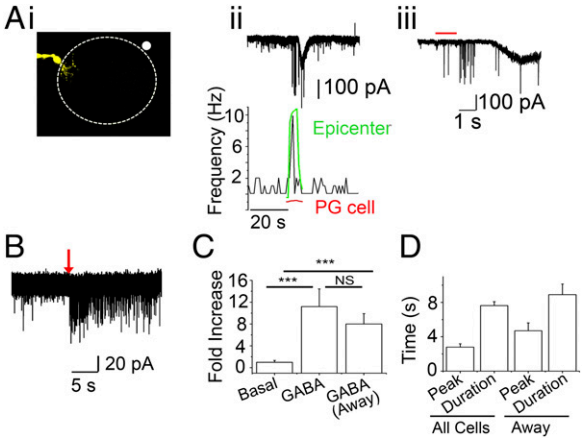

Fig. 3. GABA-induced GABA release. All experiments were performed in the presence of 10 μM DNQX and 50 μM APV with CsCl-based internal solutions. (*A*) Data from a single PG cell. 50 μM GABA, along with Alexa Fluor 594 hydrazide were applied via a puffer pipette for 1 s. (*i*) The left side of the image shows the recorded PG cell (–70 mV) filled with Alexa Fluor 488 dextran. The white circle outside the glomerular outline (top right corner) represents the epicenter of GABA plus Alexa Fluor 594 hydrazide dye application. (*ii*) (*Top*) GABA application results in a burst of sGPSCs, followed by a slow GABAergic current that is superimposed by sGPSCs in the recorded PG cell. (*Bottom*) Frequency plot (aligned to *Top*) representing the change in sGPSC frequency on GABA application. The green trace shows changes in Alexa Fluor 594 fluorescence at the white circle in *i* (epicenter). The red trace represents the relative change in fluorescence at the dendritic arbor of the recorded PG cell (PG cell). The rising phase of the green trace corresponds to the initial burst of sGPSCs detected by the recorded PG cell. The PG cell exhibits a delayed current corresponding with the small, slow rise in Alexa Fluor 594 fluorescence at the dendritic arbor as seen with the red trace. (*iii*) Expanded trace from *ii* showing onset delay. The red bar represents the duration of GABA application (1 s). (*B*) Another recorded PG cell showing a long-lasting barrage of sGPSCs on distant application of GABA for 3 s with no direct whole-cell GABAergic currents. (*C*) Mean sGPSC frequency (fold increase) on GABA application from all cells (n = 23; $P < 0.005$, basal vs. GABA) and from cells showing no direct GABA currents (away; n = 6; $P < 0.002$, basal vs. GABA, paired t test). (*D*) Mean sGPSC plot for time to peak (peak) and duration in local and away GABA applications. These parameters were similar in the two application modes.

the difference in time to peak for the frequency increase also did not reach statistical significance (2.7 ± 0.37 vs. 4.7 ± 0.9 s; P = 0.08, near vs. far). These results provide evidence supporting GIGR as a potential mechanism for amplifying GABA release in the glomerulus, and also suggest a role for PG–PG interactions in regulating inhibition in this microcircuit.

nAChRs Modulate GABAergic Signaling Between PG Cells. Are PG–PG synapses activated during OB signaling? Although dendrodendritic signaling between PG cells has been demonstrated (8, 9), the context in which these synapses are activated remains unclear. In previous work, we showed that activation of nAChRs in the glomerulus elicits excitation-dependent GABA release from PG cells, leading to the filtering out of MC responses to low-intensity stimuli while maintaining effective information transfer at high stimulus intensities (10, 18, 19).

We asked whether PG–PG interactions are triggered by nAChR activation. In this experiment, PG cells were held under whole-cell voltage-clamp. The pipette solution contained 200 μM Alexa Fluor 488 dextran to allow for post hoc identification of the recorded cells. A 5-s application of 1 mM ACh in the presence of 2 μM atropine (ACh/At) did not result in discernible whole-cell currents from PG cells; however, it did result in a barrage of sGPSCs (Fig. 4*A*). The mean frequency of sGPSCs rose from 0.88 ± 0.21 Hz to 9.36 ± 1.93 Hz (n = 31; $P < 0.0001$, paired t test). Similarly, on application of 5 μM nicotine, mean GPSC frequency in PG cells rose from 0.93 ± 0.45 Hz to 4.73 ± 1.09 Hz (n = 10; $P < 0.005$), confirming the nicotinic nature of the responses. nAChR-driven sGPSC bursts also were confirmed by measurements from an optogenetic mouse model, where the expression of channelrhodopsin-YFP fusion protein is driven by the choline acetyltransferase promoter (ChAT-ChR2 mice). OB slices from ChAT-ChR2 mice were incubated in 2 μM atropine. Ten pulse (10 ms/pulse) stimulations of 473-nm light, delivered at 10 Hz, resulted in a brief burst of sGPSCs on PG cells (mean frequency, 0.77 ± 0.3 Hz basal to 4.6 ± 1 Hz on stimulation; n = 9; $P < 0.005$, paired t test) (Fig. 4*A*, *iv* and *v*). The mean duration of the sGPSC burst was 3.2 ± 0.6 s, and mean onset delay was 0.5 ± 0.3 s. The kinetics of the sGPSCs were fast (Fig. 4*A*, *iv*), consistent with synaptic events rather than the slow self-inhibitory currents reported on PG cells (8, 9). Taken with the delays observed, thes findings argue for signaling across PG cells via a multistep process. Consistent with our findings that the effects of glomerular nAChR are mediated by heteromeric nAChR subtypes, the increase in sGPSC frequency was blocked by low micromolar concentrations of mecamylamine (Mec). nAChR-driven sGPSC frequency increases were abolished by 5 μM Mec (91.2% blockade; n = 5; $P < 0.02$, paired t test) (Fig. 4*B*).

In nine determinations from three PG cells, the ACh/At-driven increases in sGPSC frequencies were completely abolished by incubating slices in the presence of 10 μM DNQX, 100 μM APV, and 0.5–1 mM MCPG ($P < 0.0001$, Kolmogorov–Smirnov test of interevent interval distributions for ACh/At alone and ACh/At in the presence of GluR blockers) (Fig. 4*C*). This is similar to the data obtained on nAChR-mediated increases in sGPSC frequencies on MCs and ET cells (10, 19) and suggests that the GABAergic signaling in these neurons in the glomerular microcircuit is secondary to excitation and glutamate release, presumably from nAChR-mediated activation of MCs and ET cells.

Our data suggest that PG–PG signaling plays a role in nAChR modulation of glomerular output. Is this interaction a part of the olfactory circuitry activated by ON inputs, or is it recruited only during nAChR modulation? Using OMP-ChR2 mice, we show that PG–PG synapses can be activated by ON stimulation (Fig. S3). A brief 10-Hz stimulation resulted in a single excitatory postsynaptic current (EPSC) or a brief burst of asynchronous EPSCs on PG cells (Fig. S3*A*, *i*). On average, the delay between the onset of the stimulus and the first EPSC was 9.2 ± 2 ms (n = 6). At the same time, a delayed barrage of sGPSCs was observed on

NEUROSCIENCE

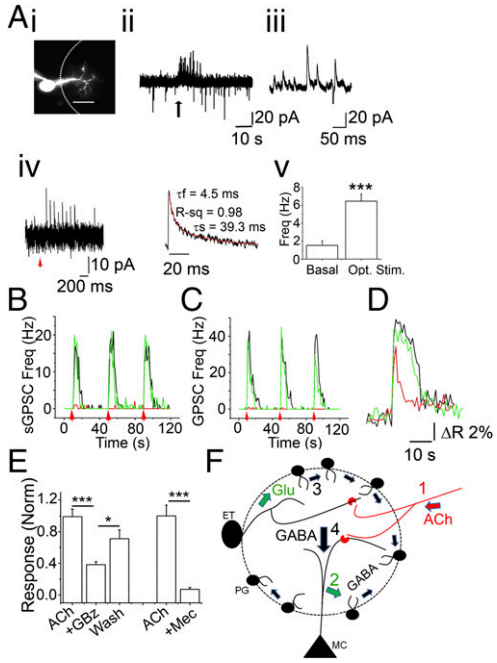

Fig. 4. nAChR activation results in glutamate-dependent increase in the frequency of sGPSC on PG cells. (*A*) (*i*) A PG cell loaded with Alexa Fluor 488 dextran to identify its dendritic arborization within a glomerulus. (Scale bar: 10 μm.) (*ii*) A 5-s application of 1 mM ACh/At at the arrow results in a barrage of sGPSCs recorded at −30 mV. (*iii*) Expanded trace showing individual sGPSCs from the barrage in *ii*. (*iv*) Recordings of a PG neuron from a ChAT-ChR2 mouse. (*Left*) Optical stimulation (473 nm) of cholinergic fibers for 10 ms at 10 Hz results in a barrage of sGPSCs in the recorded PG cell. (*Right*) Expanded example of an averaged sGPSC from *iv*. (*v*) Averaged sGPSC frequencies under basal (basal) and stimulated (opt. stim.) conditions (n = 9; $P < 0.005$, paired *t* test). (*B*) Frequency plot representing sGPSC frequency change owing to ACh/At applications (red arrows) control (black), 5 μM Mec (red), and wash (green). ACh/At-mediated increase in sGPSC frequencies arises from activation of heteromeric nAChRs. Mec abolishes nAChR-mediated increases in sGPSC frequencies. (*C*) Frequency plot representing sGPSC frequency change owing to ACh/At applications (red arrows) in control (black), GluR blockers (red), and wash (green). GluR blockers (20 μM DNQX + 100 μM D-APV +1 mM MCPG) reversibly abolish ACh/At-induced barrage of sGPSCs at −30 mV. (*D*) Calcium transient from a JG neuron in response to 1 mM ACh/At. The agonist elicits a large calcium transient (black trace) that is significantly attenuated after application of 20 μM GBz (red trace) in a reversible manner (wash; green trace), consistent with the idea that nAChR-dependent GABA release contributes to PG cell calcium signals. (*E*) Compiled data from 24 cells from three experiments showing response to nAChR activation (ACh), block by 20 μM GBz (GBz), and washout (wash). $***P < 10^{-8}$, ACh vs. +GBz; $*P < 0.05$, +GBZ vs. wash. Similarly the nAChR-mediated calcium transients were blocked by 5 μM Mec (+Mec). $***P < 10^{-5}$. Significance was calculated using the paired *t* test. (*F*) A model for GIGR. Functional nAChRs (red crescents) are expressed on MC primary dendrites and on ET cells (10, 19). Release of ACh from basal forebrain cholinergic neurons (red; 1) activates the nAChRs, resulting in glutamate release onto a population of PG cells (green; 2). Excitation of PG cells in turn releases GABA on to adjacent PG cells, resulting in propagation of this excitation via GIGR (black, small arrows; 3). This results in amplified GABA release and inhibition of all MCs in the microcircuit (black, large arrow; 4), filtering weak inputs from the ON. Runaway excitation of PG cells is prevented by $GABA_A$R-mediated inhibition of PG cell firing, thereby establishing a finite set point for glomerular inhibition.

ON stimulation, when the cell was held at 0 mV (Fig. S3*A*, *i*). The mean delay to the first sGPSC was 15 ± 2.6 ms ($n = 6$). Increases in sGPSC frequencies were observed both in cells that showed discernible EPSCs on ON stimulation and those that did not (Fig. S3 *A*, *i* and *B*). The average sGPSC frequency on stimulation (measured from onset to a 90% decay in binned frequency distribution; Fig. S3*A*, *iii*) was 2.7 ± 0.5 Hz ($n = 16$). The average peak frequency was 7.2 ± 1.2 Hz, and the average duration of the sGPSC burst was 4.76 ± 0.5 s ($n = 6$ cells). The mean frequency increase was lower when the ON was stimulated with low frequencies (two pulses at 2 Hz; 0.9 ± 0.3 Hz; $n = 13$; $P < 0.01$) (Fig. S3*D*).

As expected, the increase in sGPSCs on PG cells after ON stimulation was excitation-driven, presumably via glutamate release onto PG cells from the ON, ET cells, or MCs. Incubating the slices with 10 μM DNQX and 50 μM APV abolished the OMPChR2-driven increase in sGPSC in a reversible manner (89.4% block; n =4; $P < 0.05$) (Fig. S3 *A*, *iii* and *C*).

Based on the GluR-dependence of the GPSC increase in PG cells during both nAChR modulation and ON stimulation, we predicted that activation of nAChRs should increase glutamate release onto PG cells as well. We measured changes in the frequencies of glutamatergic synchronous EPSCs (sEPSCs) on nAChR activation in PG neurons. Surprisingly, only a fraction of PG cells (~35%; 16 out of 46 cells) that we recorded from exhibited a significant increase in the frequency of sEPSCs on focal application of 1 mM ACh/At (Fig. S4; significance for increases in individual cells established by the Kolmogorov–Smirnov test for interevent intervals between sGPSCs). Whether this reflects the reported heterogeneity in glutamatergic inputs onto the PG cells (20, 21) remains to be determined. For cells exhibiting a significant increase in sEPSCs, the mean sEPSC frequency increased from 1.52 ± 0.46 Hz to 11.05 ± 2.25 Hz ($n = 16$; $P < 0.001$, paired *t* test). This ACh-mediated increase in sEPSC frequencies in PG cells was also abolished by 5 μM Mec (92.6% blockade for sEPSCs; $n = 5$; $P < 0.05$, paired *t* test). Cells that showed sEPSC frequency increases also showed robust bursts of sGPSCs (included in the aforementioned analyses of the sGPSC effects).

The involvement of PG–PG signaling in nAChR modulation implies that GIGR could serve as a means of amplifying glomerular inhibition in response to receptor activation (Fig. 4*F*). If this is the case, then a simple prediction, based on our data obtained thus far, would be that $GABA_A$Rs contribute to nAChR-mediated calcium transients in JG neurons. Calcium transients in response to 1 mM ACh/At were recorded from JG neurons from slices loaded with fura-2AM. Consistent with the data presented above and previous laboratory work (10, 19), activation of nAChRs produced robust calcium transients that were blocked on incubation with 5 μM Mec (86 ± 5.6% block; $n = 35$ cells; $P < 10^{-5}$, paired *t* test) (Fig. 4*E*). Importantly, 20 μM GBz significantly blocked nAChR-mediated increases in $[Ca]_i$ (Fig. 4*D*). From a total of 38 cells from three experiments, loaded with fura-2AM, 24 cells showed a decrease in 100 μM ACh/At-mediated ΔR in the presence of GBz (mean inhibition, 61% ± 3.8%; $P < 10^{-8}$, paired *t* test) (Fig. 4*E*). A small fraction of the JG neurons showed an increase in response to the $GABA_A$R block (response in the presence of the blocker, 190% ± 50% of ACh/At alone; $n = 5$, $P < 0.05$) (Fig. 4*E*). Whether these results indicate tonic inhibition by GABA of ET cells and other non-PG cells in the glomerulus or is a consequence of the bimodality of GABAergic effects on PG cells remains to be determined. Our findings suggest that GABA release from JG neurons contributes to nAChR-mediated calcium transients, consistent with the idea that GIGR can serve to amplify glomerular inhibition in response to circuit excitation.

Discussion

This study makes two important observations. The first of these is that PG–PG interactions are prevalent in the glomerular microcircuitry. Models of OB function need to incorporate these synapses and their unique ability to dynamically regulate glomerular inhibition. The combination of excitatory GABA and GIGR provides a previously unidentified mechanism for the regulation of the transfer function across the glomerulus. The second observation is that these interactions participate in modulation by cholinergic centrifugal inputs.

Connections between GABAergic interneurons are thought to play a role in shaping spatial and temporal features of circuit

inhibition (22, 23). In the OB, the existence of PG–PG synapses has been demonstrated (8, 9) although whether, or how, they might participate in altering input–output functions of the glomerular microcircuit is not known. Our results paint a complex picture of GABAergic signaling among these neurons. We show that in PG cells, GABA is excitatory or inhibitory depending on the activity state of these cells. In acute slices, as has been suggested from studies in vivo, PG cells exhibit very little if any spontaneous activity (11, 12). Under these conditions, GABA drives the cells above their firing threshold. In contrast, if PG cells are tonically active, then GABA inhibits firing either by shunt inhibition or by hyperpolarization.

The bidirectionality of GABA action could serve to buffer firing rates of PG cells and to set thresholds for glomerular inhibition, thereby acting as a tunable filter for incoming odor inputs. Thus, the consequences of activation of the PG network could range from inhibition of MCs to disinhibition, based on the activity history of the microcircuit.

The variable and diffuse cholinergic projections from the basal forebrain (24, 25) and the lack of specific topography within the horizontal limb of the diagonal band of Broca suggest that cholinergic modulation occurs across the bulb, rather than in a glomerular- or odor-specific manner. Such an arrangement points to control of more global arousal/attentional processes (26, 27) than specific odor-driven modulation. Studies measuring ACh levels in real time in actively behaving mice that show a large spike in ACh levels (lasting a few seconds) during the attentional/anticipation phase (28, 29) support this view.

In the glomerulus, functional nAChRs are expressed on MCs and ET cells. Arrival of cholinergic input would excite these cells, setting up a period of inhibition via PG cell-mediated GABA release (Fig. 4*F*). Consequent GIGR serves to ensure uniform inhibition of all MCs belonging to a glomerulus, thereby setting up an effective inhibitory threshold for information transfer. Any odor input arriving within this period will be subject to a filtering effect whereby weak inputs result in failures. The duration of this effect would be the combination of the duration of ACh release, nAChR desensitization, and GIGR.

The cholinergic effect would be odor-independent and occur at all glomeruli. Bimodal regulation of PG cells by GABA would allow for consistency in the filter threshold, normalizing for variability in activity between glomeruli, at any given point in time. Differential control might depend simply on open conductance and shunting; however, rapid and transient (at a millisecond to second time scale), activity-dependent shifts in E_{GABA} have also been reported from interneurons (30).

The various parameters that are modulated to allow for such bidirectional control of circuit excitability in the CNS remain to be elucidated. In the glomerular microcircuit, PG–PG interactions need to be taken into account to understand olfactory information transfer.

Methods

FVB mice (12–16 d old, from Charles River Laboratories) were used for most of the experiments. ChAT-ChR2EYFP mice were obtained by breeding a ChATCre line (B6;129S6-*ChAT*$^{tm2(cre)Lowl}$/J; The Jackson Laboratory) with a Rosa ChR2 line (B6;129S-*Gt(ROSA)26Sor*$^{tm32(CAG-COP4*H134R/EYFP)Hze}$/J; The Jackson Laboratory). Olfactory Marker Protein-ChR2 (OMP-ChR2) mice, obtained from D. Restrepo at the University of Colorado School of Medicine (31) were used for the optical stimulation experiments. All experiments were carried out using protocols approved by the Institutional Animal Care and Use Committee of the University of Colorado Anschutz Medical Campus. Details are provided in *SI Methods*.

ACKNOWLEDGMENTS. We thank Dr. Diego Restrepo at the University of Colorado School of Medicine and Dr. Thomas Bozza at Northwestern University for use of the OMPChR2 mice. Funding for this study was provided by the National Institute on Deafness and Other Communication Disorders (Grant R01 DC 008855, to S.V.).

1. Pouille F, Scanziani M (2001) Enforcement of temporal fidelity in pyramidal cells by somatic feed-forward inhibition. *Science* 293(5532):1159–1163.
2. Higley MJ, Contreras D (2006) Balanced excitation and inhibition determine spike timing during frequency adaptation. *J Neurosci* 26(2):448–457.
3. Marty A, Llano I (2005) Excitatory effects of GABA in established brain networks. *Trends Neurosci* 28(6):284–289.
4. Delpire E (2000) Cation–chloride cotransporters in neuronal communication. *News Physiol Sci* 15:309–312.
5. Ben-Ari Y (2002) Excitatory actions of GABA during development: The nature of the nurture. *Nat Rev Neurosci* 3(9):728–739.
6. Gulledge AT, Stuart GJ (2003) Excitatory actions of GABA in the cortex. *Neuron* 37(2):299–309.
7. Chavas J, Marty A (2003) Coexistence of excitatory and inhibitory GABA synapses in the cerebellar interneuron network. *J Neurosci* 23(6):2019–2031.
8. Murphy GJ, Darcy DP, Isaacson JS (2005) Intraglomerular inhibition: Signaling mechanisms of an olfactory microcircuit. *Nat Neurosci* 8(3):354–364.
9. Smith TC, Jahr CE (2002) Self-inhibition of olfactory bulb neurons. *Nat Neurosci* 5(8):760–766.
10. D'Souza RD, Vijayaraghavan S (2012) Nicotinic receptor-mediated filtering of mitral cell responses to olfactory nerve inputs involves the α3β4 subtype. *J Neurosci* 32(9):3261–3266.
11. Homma R, Kovalchuk Y, Konnerth A, Cohen LB, Garaschuk O (2013) In vivo functional properties of juxtaglomerular neurons in the mouse olfactory bulb. *Front Neural Circuits* 7:23.
12. Wachowiak M, et al. (2013) Optical dissection of odor information processing in vivo using GCaMPs expressed in specified cell types of the olfactory bulb. *J Neurosci* 33(12):5285–5300.
13. Angelo K, et al. (2012) A biophysical signature of network affiliation and sensory processing in mitral cells. *Nature* 488(7411):375–378.
14. Holderith NB, Shigemoto R, Nusser Z (2003) Cell type-dependent expression of HCN1 in the main olfactory bulb. *Eur J Neurosci* 18(2):344–354.
15. Harris NC, Constanti A (1995) Mechanism of block by ZD 7288 of the hyperpolarization-activated inward rectifying current in guinea pig substantia nigra neurons in vitro. *J Neurophysiol* 74(6):2366–2378.
16. Gasparini S, DiFrancesco D (1997) Action of the hyperpolarization-activated current (I_h) blocker ZD 7288 in hippocampal CA1 neurons. *Pflugers Arch* 435(1):99–106.
17. Staley K, Smith R (2001) A new form of feedback at the GABA(A) receptor. *Nat Neurosci* 4(7):674–676.
18. D'Souza RD, Vijayaraghavan S (2014) Paying attention to smell: Cholinergic signaling in the olfactory bulb. *Front Synaptic Neurosci* 6:21.
19. D'Souza RD, Parsa PV, Vijayaraghavan S (2013) Nicotinic receptors modulate olfactory bulb external tufted cells via an excitation-dependent inhibitory mechanism. *J Neurophysiol* 110(7):1544–1553.
20. Gire DH, Schoppa NE (2009) Control of on/off glomerular signaling by a local GABAergic microcircuit in the olfactory bulb. *J Neurosci* 29(43):13454–13464.
21. Kiyokage E, et al. (2010) Molecular identity of periglomerular and short axon cells. *J Neurosci* 30(3):1185–1196.
22. Galarreta M, Hestrin S (2002) Electrical and chemical synapses among parvalbumin fast-spiking GABAergic interneurons in adult mouse neocortex. *Proc Natl Acad Sci USA* 99(19):12438–12443.
23. Tamás G, Somogyi P, Buhl EH (1998) Differentially interconnected networks of GABAergic interneurons in the visual cortex of the cat. *J Neurosci* 18(11):4255–4270.
24. Zheng LM, Ravel N, Jourdan F (1987) Topography of centrifugal acetylcholinesterase-positive fibres in the olfactory bulb of the rat: Evidence for original projections in atypical glomeruli. *Neuroscience* 23(3):1083–1093.
25. Salcedo E, et al. (2011) Activity-dependent changes in cholinergic innervation of the mouse olfactory bulb. *PLoS One* 6(10):e25441.
26. Sarter M, Bruno JP, Givens B (2003) Attentional functions of cortical cholinergic inputs: What does it mean for learning and memory? *Neurobiol Learn Mem* 80(3):245–256.
27. Sarter M, Hasselmo ME, Bruno JP, Givens B (2005) Unraveling the attentional functions of cortical cholinergic inputs: Interactions between signal-driven and cognitive modulation of signal detection. *Brain Res Brain Res Rev* 48(1):98–111.
28. Parikh V, Sarter M (2008) Cholinergic mediation of attention: Contributions of phasic and tonic increases in prefrontal cholinergic activity. *Ann N Y Acad Sci* 1129:225–235.
29. Parikh V, Kozak R, Martinez V, Sarter M (2007) Prefrontal acetylcholine release controls cue detection on multiple timescales. *Neuron* 56(1):141–154.
30. Isomura Y, et al. (2003) Synaptically activated Cl^- accumulation responsible for depolarizing GABAergic responses in mature hippocampal neurons. *J Neurophysiol* 90(4):2752–2756.
31. Bozza T, Feinstein P, Zheng C, Mombaerts P (2002) Odorant receptor expression defines functional units in the mouse olfactory system. *J Neurosci* 22(8):3033–3043.
32. Kosaka T, Kosaka K (2005) Structural organization of the glomerulus in the main olfactory bulb. *Chem Senses* 30(Suppl 1):i107–i108.
33. Kosaka T, Kosaka K (2011) "Interneurons" in the olfactory bulb revisited. *Neurosci Res* 69(2):93–99.
34. Ghatpande AS, Sivaraaman K, Vijayaraghavan S (2006) Stored calcium mediates cholinergic effects on mIPSCs in the rat main olfactory bulb. *J Neurophysiol* 95(3):1345–1355.
35. Lu T, Trussell LO (2001) Mixed excitatory and inhibitory GABA-mediated transmission in chick cochlear nucleus. *J Physiol* 535(Pt 1):125–131.
36. Perkins KL (2006) Cell-attached voltage-clamp and current-clamp recording and stimulation techniques in brain slices. *J Neurosci Methods* 154(1-2):1–18.
37. Sharma G, Grybko M, Vijayaraghavan S (2008) Action potential-independent and nicotinic receptor-mediated concerted release of multiple quanta at hippocampal CA3-mossy fiber synapses. *J Neurosci* 28(10):2563–2575.